Shackleton, N.J., Curry, W.B., Richter, C., and Bralower, T.J. (Eds.), 1997
Proceedings of the Ocean Drilling Program, Scientific Results, Vol. 154

12. CARBONATE PRODUCTION AND DISSOLUTION IN THE WESTERN EQUATORIAL ATLANTIC DURING THE LAST 1 M.Y.[1]

W.B. Curry[2] and J.L. Cullen[3]

ABSTRACT

Variations in calcium carbonate sedimentation on Ceara Rise have been dominated by dilution of noncarbonate material derived from the Amazon. There has been a continuous increase in the input of this material during the last 1 m.y., which may be related to a long-term increase in erosion in the Amazon drainage basin. In addition, large glacial-interglacial differences in carbonate concentration are caused mainly by increased dilution by noncarbonate material during low sea levels. In the shallowest sites, long-term average carbonate accumulation has been relatively constant, suggesting that average carbonate productivity has been constant. But there are indications that accumulation has varied on shorter time scales: a prominent maximum at about 410 ka, for instance, exhibits accumulation rates that are twice the average value. Bathymetric differences in carbonate accumulation imply that dissolution was more severe in the deepest site prior to about 433 ka. Throughout the last 1 m.y., carbonate accumulation rates and concentrations have been converging toward similar values at all water depths, implying that the bathymetric gradient in [CO_3^{-2}], which marks the transition from North Atlantic Deep Water to Circumpolar Deep Water, has been reducing. Therefore, the calcite saturation levels of the two water masses have become more similar over the last 1 m.y.

INTRODUCTION

One of the principal goals of Leg 154 was to recover a depth transect of cores from the Ceara Rise in order to reconstruct the Cenozoic history of carbonate dissolution and production in the western equatorial Atlantic. The depth transect approach was used because it provides important constraints on the several parts of the carbonate system. First, the shallowest cores on the rise are the ones least likely to have been affected by dissolution and are therefore best representative of the original input signal of carbonate production from surface waters. Particles deposited above the lysocline undergo dissolution only to the extent that degradation of organic carbon may drive dissolution within pore waters. Second, the sites of the depth transect are located close to one another, and downslope reworking of material is limited. As a result, the input of carbonate from above is the same in each site, and the differences among the sites result only from loss of carbonate from dissolution. Finally, the input of noncarbonate material provides some constraint on the lateral movement of particles. The extent that terrigenous fluxes differ among the sites is indicative of the physical movement of material by bottom current erosion, hemipelagic redeposition, and downslope reworking.

The sites recovered during Leg 154 present an opportunity to reconstruct this history of carbonate production and dissolution for at least the last 5 m.y. The purpose of this paper is to present this history for the last 1 m.y., the period during which the Earth's climate changed from one with an obliquity response to orbital forcing to one with an eccentricity response.

STUDY AREA

The Ceara Rise is overlain by the two principal deep water masses in the western North Atlantic, North Atlantic Deep Water (NADW) from the top of the rise down to about 4100 m and Lower Circumpolar Deep Water (CPDW) below 4100 m. The water mass boundary is marked by a transition from the warmer, saltier NADW that is saturated with respect to calcite to colder, fresher CPDW that is undersaturated with respect to calcite (Curry, Shackleton, Richter, et al., 1995). The [CO_3^{-2}] gradient between the water masses today is about 10 µmol/kg. The five sites recovered during Leg 154 operations spanned these water depths, so the sites are nearly ideally located for reconstructing past changes in the interactions of these water masses and any changes in their chemistry. Surface water hydrography above Ceara Rise is typical of the warm tropics, with low seasonal variation in sea surface temperature (SST) and a mean SST of about 27°C. The mixed layer is generally thick (>100 m); low nutrient concentrations in surface waters and little upwelling lead to generally low productivity. Sedimentation rates in this region are elevated, however, because of detrital input from the nearby Amazon Fan. Consequently, the geological record in this region can be highly resolved despite the generally low surface water productivity. Ceara Rise is also a region where the assumption of nutrient limitation in surface waters is sound, so the production rate of carbonate will be limited by the delivery of nutrients to the mixed layer.

METHODS

Samples for this study were taken at a 10-cm spacing from the composite depth sections constructed during shipboard operations of Leg 154. Small aliquots of samples were separated from the main bulk of the sample and used for analysis of calcium carbonate concentration. The remaining samples were soaked in a calgon-hydrogen peroxide solution and processed for taxonomic and stable isotopic analysis (see Cullen and Curry, this volume). The carbonate samples were dried and weighed, and their carbonate concentration was determined based on the gas pressure evolved from their reaction with phosphoric acid in a constant volume system (Ostermann et al., 1990). Replicate analyses of carbonate samples document that the reproducibility of the measurement for this system is 1%. Carbonate variations in these records exceed 50%, so the signal to noise ratio is very large.

Stable isotopic measurements of the planktonic foraminifer *Globigerinoides sacculifer* from Site 927 were used to provide stratigraphic and chronologic control for the carbonate records. The spec-

---

[1] Shackleton, N.J., Curry, W.B., Richter, C., and Bralower, T.J. (Eds.), 1997. *Proc. ODP, Sci. Results,* 154: College Station, TX (Ocean Drilling Program).

[2] Department of Geology and Geophysics, Woods Hole Oceanographic Institution, Woods Hole, MA 02543, U.S.A. wcurry@whoi.edu

[3] Department of Geological Sciences, Salem State College, Salem, MA 01970, U.S.A.

Previous Chapter Table of Contents Next Chapter

imens were picked from the 300- to 355-µm size fraction and analyzed using a Finnigan MAT252 mass spectrometer equipped with an automated carbonate device. Each isotopic sample was composed of seven *G. sacculifer* specimens. The samples were not roasted before analysis. The isotopic data were converted to PDB through intercalibrations with NBS19. Long-term precision of this standard for our mass spectrometer system is 0.03‰ (1σ) for $\delta^{13}C$ and 0.08‰ (1σ) for $\delta^{18}O$ for isotopic samples ($n > 1600$) with a median size of 66 µg. Precision is size dependent; for samples less than 20 µg, the precision is 2× less accurate. However, the mass of seven *G. sacculifer* tests is much greater than 100 µg, so the analytical precision we expect for these samples should be better than the quoted values.

RESULTS

Carbonate Records

Carbonate concentration is plotted vs. meters composite depth (mcd) below seafloor in Figure 1. In the shallow sites (925, 927, and 926), carbonate concentrations vary from highs of about 70% to lows of about 15%, and exhibited significant rapid transitions between the extremes. As would be expected, mean concentrations are highest in Site 925 on the top of Ceara Rise and decrease with depth in the water column (Table 1), but there are also lateral gradients in carbonate concentration caused by differences in proximity to the Amazon Fan (Fig. 2). For instance, the mean carbonate concentration of Site 927 is lower than at Site 926 despite the 300-m shallower position of Site 927 on Ceara Rise, because of a greater input of terrigenous, noncarbonate material at Site 927. This greater input of terrigenous material also affects Sites 928 and 929. Sorting out the differences in terrigenous input to the sites requires calculations of the mass accumulation rates of the sedimentary components, which we provide below. Calculating accumulation rate, in turn, requires knowledge of the sedimentation rates and bulk density of the sediments in these sites.

Stratigraphy and Chronology

The stratigraphy and chronology for our records comes from the tuned time scale produced by Bickert, Cordes, and Wefer (this volume). The time scale is based on tuning the observed variations in magnetic susceptibility within the composite section to an orbital target using an assumed 2-k.y. phase difference between the records for the entire interval from 0 to 5 Ma. Susceptibility was chosen because it and color reflectance were measured throughout the entire length of each composite section, and each exhibits large orbital variations that make tuning easy and reliable. The (as yet) incomplete stable isotopic records for each site were then compared to assure that no phase differences were introduced using this approach.

The time scales used for this paper were derived independently from the carbonate data, but carbonate concentration and magnetic susceptibility covary in these sediments. By using magnetic susceptibility records to correlate the sites, the carbonate records are forced to have the same phase. This assumption may ultimately prove to be untrue; for instance, if there is a phase difference that is a function of water depth. Full evaluation of this assumption can only be made after complete stable isotopic records have been produced for all Leg 154 sites. On the basis of the tuned time scales as used, a plot of the depth-age relationships for these sites is presented in Figure 3.

Sedimentation rates vary in these sites (Table 2) from a low of about 2.85 cm/k.y. in the lower part of Site 926 (433−1010 ka) to a high of about 4.92 cm/k.y. in the upper section of Site 927 (0−433 ka). The sites closest to the Amazon Fan (Sites 927, 928, and 929) have average sedimentation rates that are about 10% higher than the southern sites (Sites 925 and 926). Sedimentation rates at each site have been fairly uniform for long periods, but there was an important change in rate observed at about 433,000 yr ago. At this time, sedimentation rates increased at all sites by about 35%.

Time-Depth Variations in Carbonate

The carbonate concentration records are plotted vs. age in Figure 4. The sites are ranked on the figure by water depth with the shallowest in the water column at the top of the figure. Short-term variations in carbonate concentration, on the scale of 10^4–10^5 years, can be traced throughout the entire water column. There is, however, a shift toward lower mean values with increasing water depth. In Site 925, for instance, carbonate concentration varies from lows of about 20 during glacial maxima to highs of about 70% during interglacials. At Site 929, however, low values are often close to 0% and high values rarely exceed 60%. Despite the differences in range, prominent maxima in carbonate concentration are found at all water depths. The three shallowest sites (925, 927, and 926) exhibit very similar variability over this interval, with the differences among these sites a shift toward lower values in Site 927 because of its closer proximity to the Amazon Fan. Sites 928 and 929 differ from the others in their tendency toward much lower values during prominent glacial maxima.

There are also secular trends in the carbonate concentration data that imply long-term changes in the corrosiveness of the deep waters in this region (Fig. 5). Linear regressions of carbonate concentration vs. age document that the four shallowest sites have experienced a gradual reduction in carbonate concentration of about 5%−10% during the last 1 m.y. This gradual decrease is part of a longer term trend that was observed by the shipboard scientific party, which they attributed to an increasing input of Amazon-derived detrital material (Curry, Shackleton, Richter, et al., 1995). Interestingly, the pattern in the deepest site is not the same. The four shallowest sites all decrease in parallel throughout the last 1 m.y., offset only by their mean values. The deepest site, however, increased during this period by about 5%. Thus, carbonate concentrations have become more uniform throughout the water column. If this change was not caused by differences in the regional patterns of noncarbonate dilution, then there has been a change in the relative corrosiveness of the water masses in this region. Today the CPDW:NADW boundary marks the transition from undersaturation to supersaturation with respect to calcite. If these water masses have both been present and interacting in this region throughout the last 1 m.y., the implication of the patterns in Figure 5 is that the difference in the corrosiveness of the water masses has decreased toward the present. One interpretation of this is that there has been a change in the carbon chemistry of the two water masses; the carbonate ion concentration gradient must have decreased over the past 1 m.y. Benthic foraminiferal $\delta^{13}C$ records at these sites should also converge toward more similar values over this period of time. (The data to test this prediction were not ready for publication within the schedules of ODP publication policy.)

Carbonate and Ice Volume Variations

Both the carbonate and $\delta^{18}O$ records for *G. sacculifer* exhibit significant variability at the primary orbital periods and for shorter periods as well (Figs. 6, 7). Using the Multitaper Power Spectral Method of Thompson (1990), we observed significant periodic behavior in these records over a wide range of frequencies. The power spectral density of carbonate concentration contains nearly equal energy at the primary Milankovitch periods. Like other stable isotopic records, $\delta^{18}O$ of *G. sacculifer* exhibits a higher concentration of variance at the eccentricity period, with decreasing energy at the obliquity and precessional periods, respectively. For both the carbonate and $\delta^{18}O$ records, significant variance is concentrated at suborbital periods, principally 13 and 11 k.y. The carbonate concentration and $\delta^{18}O$ time series are coherent (with 95% confidence) at the primary Milankovitch periods as well as at several suborbital periods, including about 13, 11, 9.5, and 6 k.y. The extent that these suborbital variations are important for providing clues to understanding the climate system is beyond the scope of this paper, however, since evaluating these po-

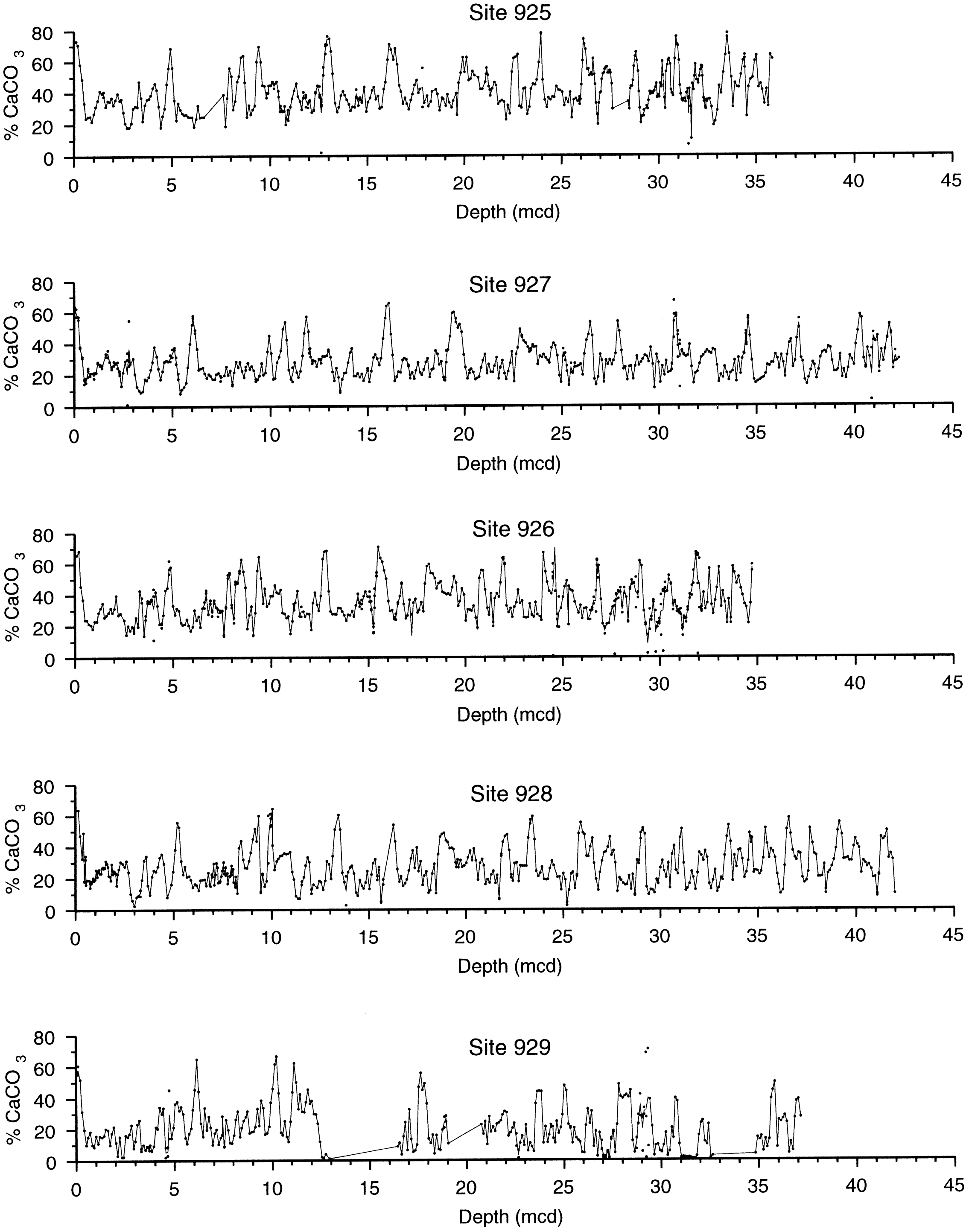

Figure 1. Percent carbonate records plotted vs. meters composite depth (mcd). The samples were taken at 10-cm intervals from the composite sections produced by the Leg 154 Shipboard Scientific Party (Curry, Shackleton, Richter, et al., 1995).

tential orbital harmonics requires more sophisticated power spectral techniques (Hagelberg et al., 1994).

Maxima in carbonate concentration lead minima in ice volume in this region at the three primary Milankovitch periods (Fig. 7). For eccentricity, the phase is about 55° (~15 k.y.); for obliquity, the phase is about 25° (~3 k.y.); and for precession, the phases are 35° (2 k.y.) for the 23 k.y. period and 7° (~0 k.y.) for the 19 k.y. period. An early response of the carbonate system was also observed by Howard and Prell (1994) for southern ocean carbonate preservation records. They noted that increased carbonate preservation led ice volume for the eccentricity and obliquity periods. Carbonate preservation also led NADW production by a larger amount at all three periods. Howard and Prell (1994) concluded that variations in deep water production alone could not have caused their observed changes in carbonate preservation. Phase relationships of carbonate preservation and deep water chemistry will be determined when the full data sets (benthic foraminiferal chemistry and planktonic foraminiferal abundance and preservation data) become available.

Table 1. Location, water depths, and mean carbonate concentration for Leg 154 sites.

Site	Latitude (N)	Longitude (W)	Water depth (m)	$CaCO_3$ (%)
925	4°12.3′	43°29.3′	3041	41.5 ± 12.6
927	5°27.8′	44°28.8′	3315	28.4 ± 10.6
926	3°43.2′	42°42.5′	3598	35.6 ± 12.4
928	5°27.3′	43°44.9′	4012	27.7 ± 12.1
929	5°58.6′	43°44.4′	4356	20.8 ± 13.9

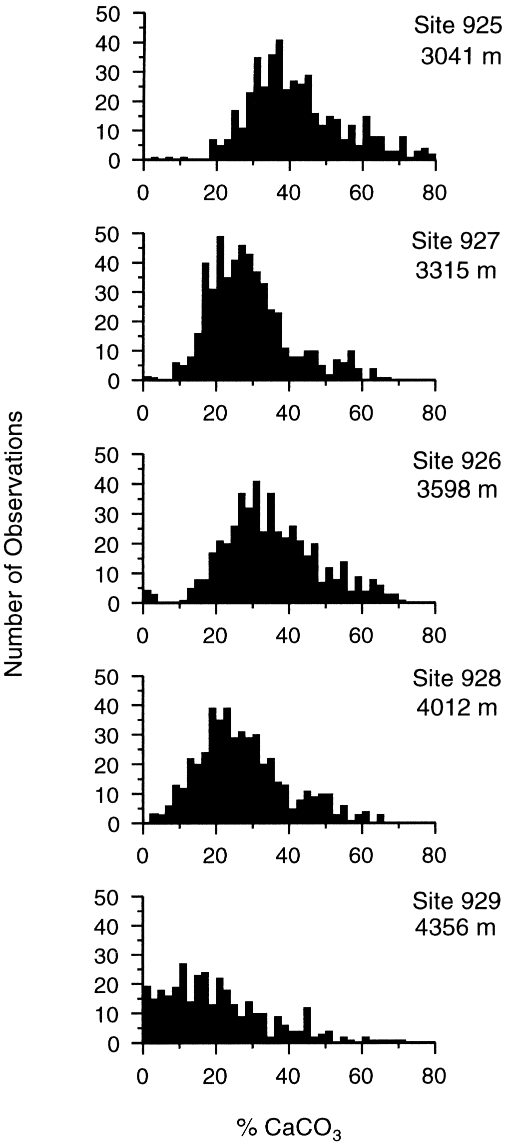

Figure 2. Histograms of carbonate concentration for Leg 154 sites. Two patterns emerge: a decrease in carbonate concentration with water depth that results from dissolution and a decrease in carbonate concentration that results from dilution by Amazon Fan terrigenous sediments. Sites 927, 928, and 929 are all from the northern part of Ceara Rise, which is in close proximity to the fan.

Carbonate Production, Dilution, and Dissolution

Accumulation rates of the carbonate and noncarbonate fractions were calculated using the measured carbonate concentration, the sedimentation rate, and an estimate of the dry bulk density. The product of these three measures equals the accumulation rate in g cm^{-2} $k.y.^{-1}$ Carbonate concentration (weight fraction) was measured on each sample, sedimentation rate in cm $k.y.^{-1}$ (in composite depth) comes from the standard chronology presented elsewhere in this volume, and bulk density (g cm^{-1}) was calculated from the discrete samples measured by Curry, Shackleton, Richter, et al., (1995). Sedimentation rates were developed by producing only one correlation point for each precession cycle, so it is not possible to compare accumulation rates for intervals at a resolution higher than this. Thus, glacial vs. interglacial accumulation rate differences predominantly reflect variations in carbonate concentration; they should be interpreted with caution. For this study, we compare the accumulation rates before and after the large change in sedimentation rate observed at about 433 ka, since this is the largest change in sedimentation observed in the data. The temporal changes in accumulation also document patterns related to variations in dissolution and dilution on shorter time scales. Bulk density in this region does not vary as a function of carbonate concentration (Curry and Lohmann, 1990), but it is strongly affected by compaction for the depth interval of this study (Fig. 8). The site to site differences in bulk density are small, so we chose to use the relationship based on the combined sites in Figure 8. A quadratic equation was developed using all of the data in Figure 8 and it was used to calculate bulk density in each site.

The records of carbonate accumulation document that the largest contributor to variations in carbonate concentration have been variations in terrigenous supply (Table 3). On average, noncarbonate accumulation increased by about 20% after 433 ka; the shallow sites increased more than the deeper sites. This change alone lowered the carbonate concentration by about 4% on average. Noncarbonate accumulation was always higher in the deepest sites and in those sites closer to the Amazon Fan; highest noncarbonate accumulations occurred during glacial intervals (Fig. 9). During interglacials, noncarbonate accumulation was similar at shallow and deep sites, as well as at northern and southern sites. This observation suggests that lowered sea level or reduced moisture conditions in the Amazon drainage basin contributed to an increased supply of noncarbonate material in the Ceara Rise during glacial periods. It is unlikely that the variation in noncarbonate resulted from variations in opal deposition since opal concentrations are quite low in this area (Curry, Shackleton, Richter, et al., 1995). The gradual increase in noncarbonate accumulation throughout the last 1 m.y. suggests that there has been a gradual increase in the influence of hemipelagic sedimentation.

There was little difference in carbonate accumulation in the shallowest sites before and after 433 ka, suggesting that only small, long-term variations in carbonate productivity have occurred in this region (Table 3). For instance, carbonate accumulation at the shallowest site increased by about 7% after 433 ka. The extent that this reflects a change in productivity depends, of course, on the extent to which dissolution has affected the shallowest sites. As yet, we have not been able to produce quantitative indices of dissolution for these sites. Variations in carbonate accumulation that occurred on shorter time scales suggest that short-term (orbital-scale) productivity variations may have occurred (Fig. 9). For instance, there is a clear high in carbonate accumulation at all water depths at about 410 ka, followed by a secular decrease in carbonate accumulation up to the present. The maximum in carbonate accumulation was twice the average value, which can only have been caused by an increase in carbonate productivity because carbonate dissolution at these water depths is so low that reducing dissolution will have only a small effect on accumulation.

The bathymetric differences in carbonate accumulation in the deepest site present clear evidence for a change in the rate of dissolution in this region (Fig. 10). Carbonate accumulation in the deepest site increased by more than 40% after 433 ka, and this increase can only have resulted from a change in dissolution (Table 3), because the

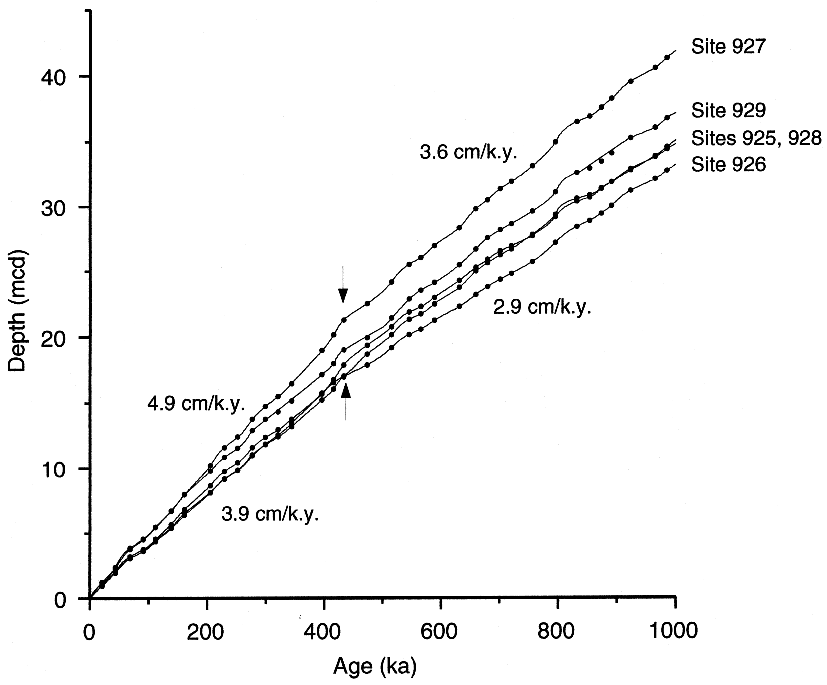

Figure 3. Depth-age curves for the Leg 154 sites. Depth is in meters in the composite depth section. The line through these data is a spline, and this mapping function was used to determine the ages of samples in the composite depth section. The largest change in sedimentation rate occurred after 433 ka. Sedimentation rates increased at that time by about 30%.

Table 2. Sedimentation rates (in cm k.y.$^{-1}$) for Leg 154 sites.

Site	0–433 (ka)	433–1010 (ka)
925	4.12	3.03
927	4.92	3.62
926	3.92	2.85
928	3.93	3.12
929	4.39	3.18

Note: There is about a 30% increase in sedimentation rate after about 433 ka. This increase resulted primarily from an increase in the input of the noncarbonate component derived from the Amazon River and fan system.

deepest site must have had the same vertical input rate of carbonate. The net change in accumulation observed in the deepest site cannot have resulted from productivity because none of the shallow sites exhibit a large increase in carbonate accumulation. Absent any change in lateral advection, the change in carbonate accumulation must have resulted from reduced dissolution in the deepest site after 433 ka. This pattern is apparent in Figure 9 as a change in the difference in carbonate accumulation between the shallowest and deepest sites. In the earlier part of the record, carbonate accumulation in the deepest sites approaches rates observed in the shallowest sites only during interglacial intervals. During glacial intervals, carbonate accumulation in the deepest site was very reduced. In the later part of the record, carbonate accumulation was much more similar at both water depths, particularly during glacial intervals. This pattern suggests that there has been reduced dissolution in this region during the last 433 ka.

DISCUSSION

The long-term decrease in carbonate dissolution in this region appears to be similar to long-term records of carbonate dissolution in the Indian Ocean (Peterson and Prell, 1985) and in the Pacific Ocean (Farrell and Prell, 1991). If it is part of a global pattern, it may have resulted from several factors. Two possibilities imply global changes in the amount of carbonate buried at shallow depths in the oceans, either on the shelves or at shallower depths in the open ocean. One of these, reduced accumulation of carbonate on continental shelf areas as sea level falls, was first pointed out by Farrell and Prell (1991). They provided this possible explanation for their observation that the depth of the carbonate compensation depth (CCD) had increased gradually during the last 4 m.y. Peterson et al. (1992) observed a similar change in the history of carbonate preservation in their synthesis of Indian Ocean drilling sites. The observations we have at Ceara Rise are consistent with this type of change in carbonate accumulation; our 1-m.y. record would be the end of a much longer global increase in carbonate preservation. Another possible mechanism that would have a similar effect on preservation in the deep ocean would be a long-term decrease in open ocean, carbonate production and, therefore, decreased burial at shallower depths (above the lysocline) in the open ocean. To balance the supply of Ca^{+2} to the oceans, burial in the deep ocean would have to increase. Consequently, preservation in the deep ocean should increase and the CCD should deepen. To separate these two possibilities, quantitative estimates of carbonate production are needed from shallow sites around the world, as well as from all continental shelf regions. The data have yet to reach this level of quality. But the Peterson et al. (1992) records from shallow Indian Ocean sites tend to support a decrease in productivity after about 3.5 Ma.

Another possible cause of this change may be a long-term change in the nutrient concentration of the deep ocean and an associated change in the carbon content of the deep ocean (Raymo et al., 1990; Farrell and Prell, 1991). On the basis of long-term records of benthic foraminiferal $\delta^{13}C$, Raymo et al. (1990) observed that the Atlantic–Pacific difference in $\delta^{13}C$ decreased by a small amount since the middle Pliocene, implying that the mean nutrient concentration of the oceans has decreased since then. This change, if accompanied by a change in the carbon content of the oceans, may be responsible for the greater dissolution observed in the Pacific Ocean during the Pliocene. The effects of this type of mechanism are not straightforward for the Atlantic, however. A larger gradient in $\delta^{13}C$ from the Atlantic to the Pacific may have caused greater dissolution in the Pacific, but less dissolution in the Atlantic would have been required to balance carbonate burial with river supply, because on long time

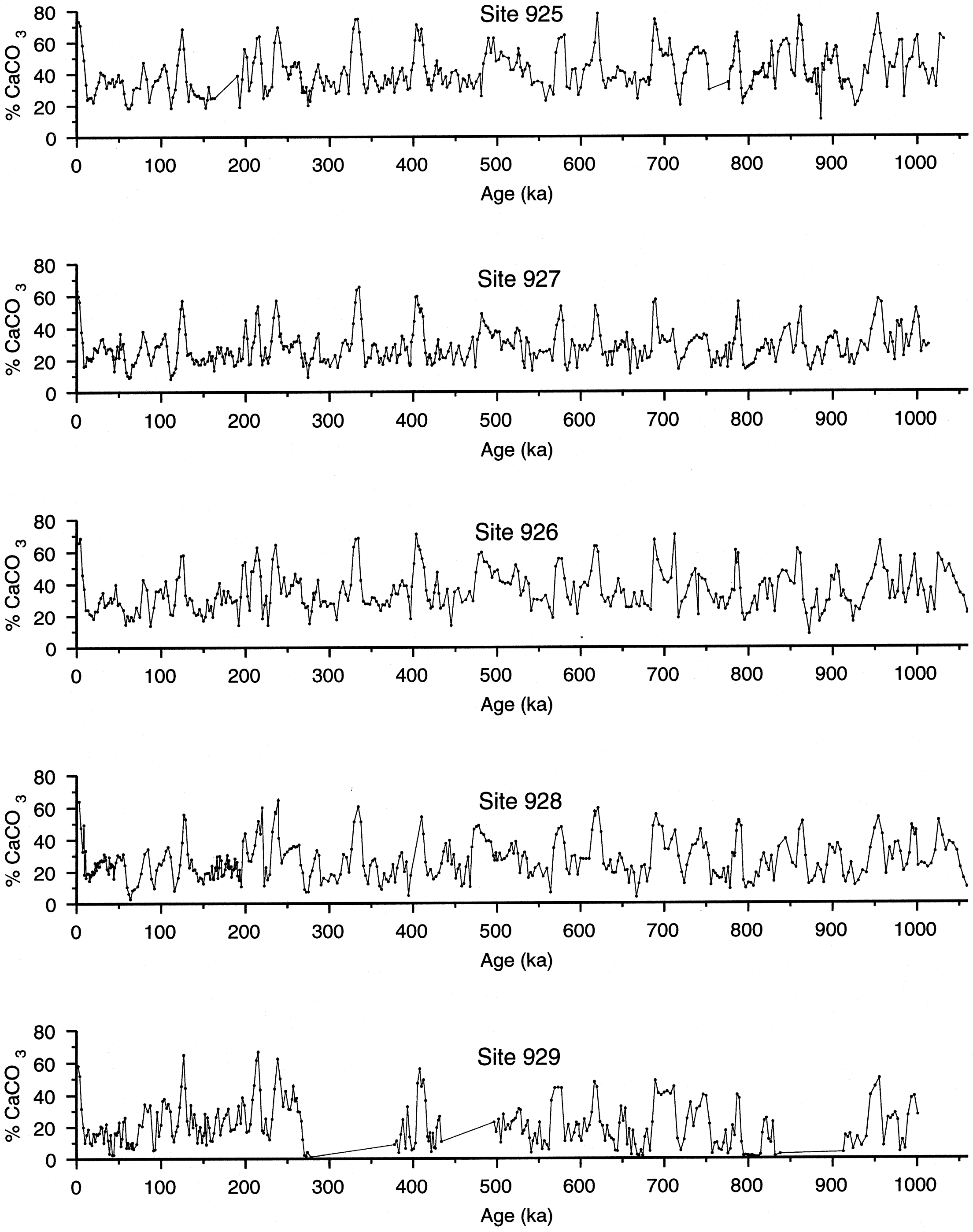

Figure 4. Percent carbonate records plotted vs. age in the composite depth section. Note that there are orbital-scale features in the records that are common at all depths. Highest carbonate concentrations occur during interglacials (see Fig. 6).

scales the burial of calcium carbonate must balance the riverine supply of calcium. But in the deepest parts of the Atlantic, where recirculated southern ocean water is flowing toward the north, a change in the corrosiveness of Pacific deep water should have an effect on dissolution. Thus, the changes we observe in the deepest Leg 154 site may have resulted from changes in the initial [CO_3^{-2}] of the deep water entering the Atlantic, which was caused by a long-term change in Pacific deep water [CO_3^{-2}]. One implication of this model is that the $\delta^{13}C$ contrast of NADW and CPDW should have decreased since the Pliocene (see Bickert, Curry, and Wefer, this volume). Another is that the preservation of carbonate in the shallower sites must have increased since the Pliocene. We will be able to test this possibility in future studies when quantitative indices of dissolution have been produced. Accumulation rate and carbonate concentration data are not sensitive enough to measure such subtle changes in preservation above the lysocline.

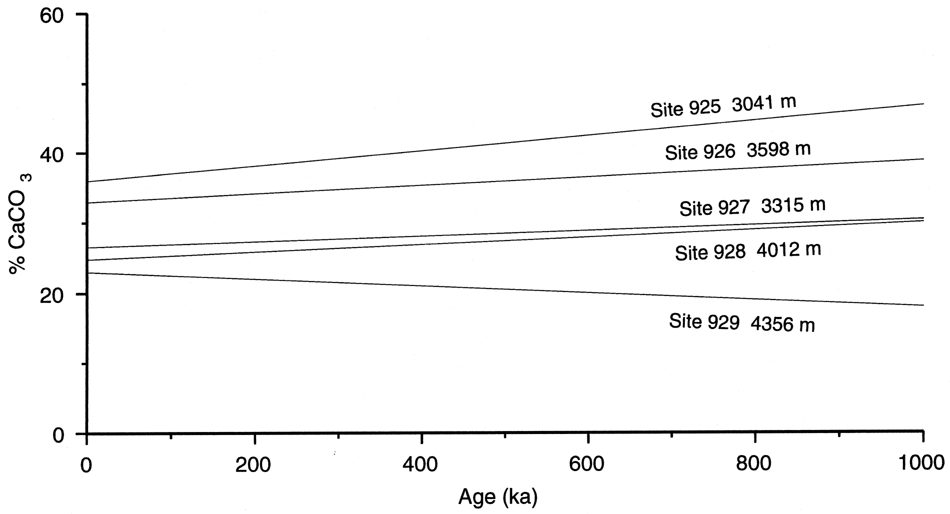

Figure 5. Linear regressions of carbonate concentration vs. age. There are two first order trends in the carbonate data: a long-term decrease in carbonate concentration in the four shallower sites and a long-term increase in carbonate concentration in the deepest site. If all sites are receiving similar input of carbonate from the surface, then this pattern must have resulted from variations in dissolution and terrigenous input. The accumulation rate data in Figures 9 and 10 suggest that a change in preservation in the deep site caused the increase in carbonate concentration.

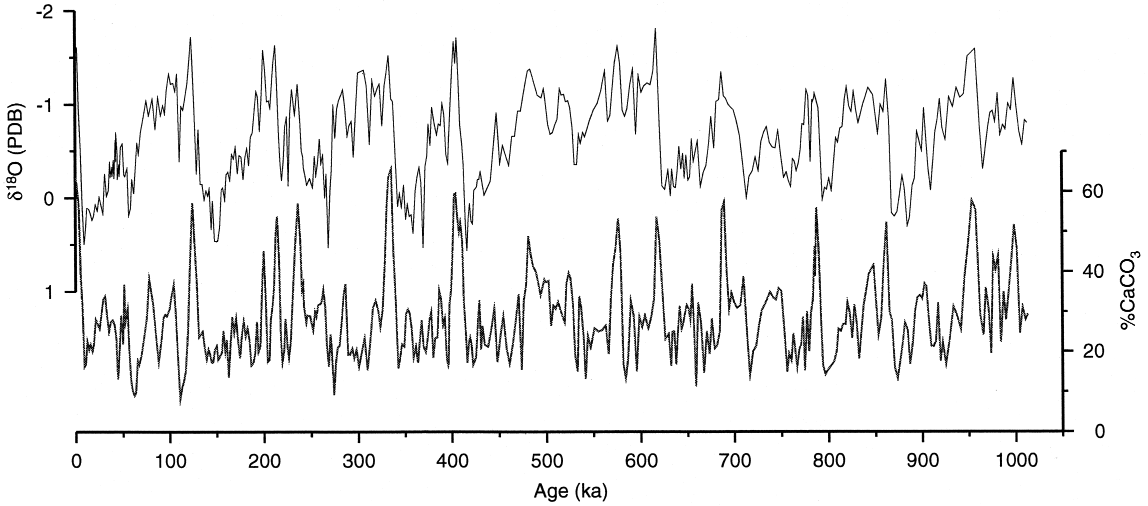

Figure 6. Carbonate concentration and *G. sacculifer* $\delta^{18}O$ records from Site 927. Lows in carbonate concentration occur during low stands of sea level and maxima in carbonate concentration lead minima in ice volume. Spectral analysis of these records suggests that the lead is 2–15 k.y., similar to the observations of other studies of long-term carbonate deposition (Peterson and Prell, 1985; Howard and Prell, 1994).

SUMMARY

1. Variations in carbonate concentration exhibit similar, orbital scale variations at all five water depths of the Leg 154 coring sites. The differences among the sites are the result of increased water depth and proximity to the Amazon Fan, both of which lower the mean carbonate concentration at a site. At the shallow sites (925, 927, and 926) carbonate concentration varies from about 15% to 70%; at the deeper sites (928 and 929) carbonate concentration varies from 0% to 60%.

2. Secular changes in carbonate concentration and accumulation during the last 1 m.y. imply that there has been increased dilution of the sediments by terrigenous material from the Amazon drainage basin. The four shallowest sites decrease in mean carbonate concentration by about 5% during this period. In contrast, the deepest site (929) increases in carbonate concentration over the same interval, implying that there has been increasing preservation of carbonate during the past 1 m.y.

3. Accumulation rate variations of carbonate imply that long-term averages in the productivity of carbonate have not varied much dur-

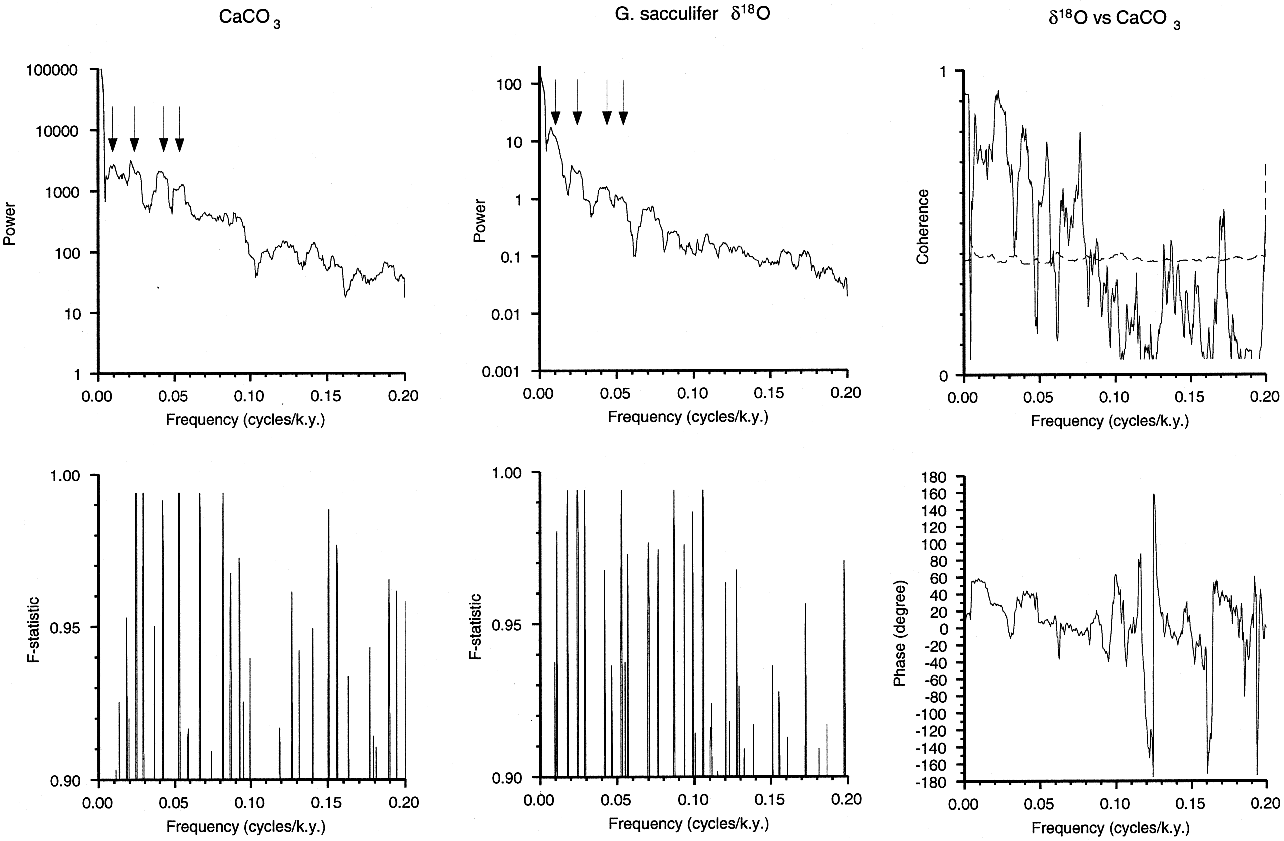

Figure 7. Multitaper spectral analysis of the carbonate and *G. sacculifer* $\delta^{18}O$ records. Significant power is present at the primary Milankovitch periods, with the carbonate record exhibiting a broader distribution of the power at higher frequencies. The arrows mark the positions of the four principal orbital frequencies. The phase plot shows that carbonate maxima lead $\delta^{18}O$ minima by 2–15 k.y.

ing the past 1 m.y., but shorter term variations were quite large. Highest productivity was about twice the mean and occurred at about 410 ka. This high in accumulation was recorded in all five Leg 154 sites. The deepest site is the only site to exhibit a long-term change in carbonate accumulation, increasing by about 40% after 433 ka. This bathymetric difference in accumulation must have resulted from a decrease in the corrosiveness of the deep water to carbonate. Because earlier glacial periods appear to have very reduced accumulation of carbonate, much of this secular change in dissolution may have been the result of a change in the corrosiveness of water penetrating to the north in the Atlantic during glacial periods.

4. The patterns observed at Ceara Rise may have been caused by global changes in the partitioning of carbonate burial among shallow and deep parts of the oceans. Or they may have resulted from changes in the initial water mass chemistry in this region. Testing these two hypotheses requires more quantitative reconstructions of global production of carbonate, dissolution at shallow depths (particularly above the lysocline), and complete benthic foraminiferal $\delta^{13}C$ records from Ceara Rise and the Pacific and Southern Oceans. These tests will be performed in future research.

ACKNOWLEDGMENTS

This paper benefited from the comments of Larry Peterson and an anonymous reviewer. We are grateful for the efforts of D.R. Ostermann in ensuring high quality and high volume data production in a very short period of time. The research was supported by National Science Foundation award OCE-9116303 to WBC and JOI/USSAC funding to WBC and JLC. This is WHOI contribution number 9206.

REFERENCES

Curry, W.B., and Lohmann, G.P., 1990. Reconstructing past particle fluxes in the tropical Atlantic Ocean. *Paleoceanography,* 5:487–505.

Curry, W.B., Shackleton, N.J., Richter, C., et al., 1995. *Proc. ODP, Init. Repts.,* 154: College Station, TX (Ocean Drilling Program).

Farrell, J.W., and Prell, W.L., 1991. Pacific $CaCO_3$ preservation and $\delta^{18}O$ since 4 Ma: paleoceanic and paleoclimatic implications. *Paleoceanography,* 6:485–498.

Hagelberg, T.K., Bond, G., and deMenocal, P., 1994. Milankovitch band forcing of sub-Milankovitch climate variability during the Pleistocene. *Paleoceanography,* 9:545–558

Howard, W.R., and Prell, W.L., 1994. Late Quaternary $CaCO_3$ production and preservation in the Southern Ocean: implications for oceanic and atmospheric carbon cycling. *Paleoceanography,* 9:453–482.

Ostermann, D.R., Karbott, D., and Curry, W.B., 1990. Automated system to measure carbonate concentration of sediments. *WHOI Tech. Rep.,* 90–103.

Peterson, L.C., Murray, D.W., Ehrmann, W.U., and Hempel, P., 1992. Cenozoic carbonate accumulation and compensation depth changes in the Indian Ocean. *In* Duncan, R.A., Rea, D.K., Kidd, R.B., von Rad, U., and Weissel, J.K. (Eds.), *Synthesis of Results from Scientific Drilling in the Indian Ocean.* Geophys. Monogr., Am. Geophys Union, 70:311–333.

Peterson, L.C., and Prell, W.L., 1985. Carbonate preservation and rates of climatic change: an 800 kyr record from the Indian Ocean. *In* Sundquist, E.T., and Broecker, W.S. (Eds.), *The Carbon Cycle and Atmospheric* CO_2*: Natural Variations Archean to Present.* Geophys. Monogr., Am. Geophys. Union, 32:251–270.

Raymo, M.E., Ruddiman, W.F., Shackleton, N.J., and Oppo, D.W., 1990. Evolution of Atlantic-Pacific $\delta^{13}C$ gradients over the last 2.5 m.y. *Earth Planet. Sci. Lett.*, 97:353–368.

Thompson, D.J., 1990. Quadratic-inverse spectrum estimates: applications to paleoclimatology. *Philos. Trans. R. Soc. London A*, 332:539–597.

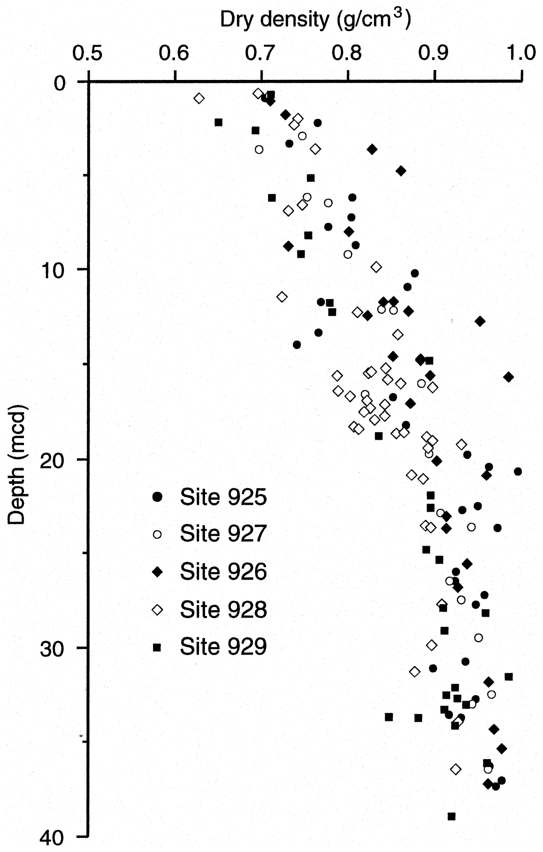

Figure 8. Dry density vs. composite depth from the shipboard observations of Leg 154 (Curry, Shackleton, Richter, et al., 1995). Compaction is the primary control of density in this region as there are only very small differences caused by variations in carbonate concentration (Curry and Lohmann, 1990).

Date of initial receipt: 4 December 1995
Date of acceptance: 7 May 1996
Ms 154SR-112

Table 3. Accumulation rates (in g cm^{-2} k.y.$^{-1}$) of carbonate and noncarbonate for Leg 154 sites.

	0–433 ka		433–1010 ka	
Site	$CaCO_3$	non-$CaCO_3$	$CaCO_3$	non-$CaCO_3$
925	1.32 ± 0.54	2.10 ± 0.60	1.22 ± 0.39	1.58 ± 0.45
927	1.12 ± 0.51	2.96 ± 0.74	1.02 ± 0.38	2.50 ± 0.63
926	1.07 ± 0.44	2.09 ± 0.53	0.98 ± 0.34	1.70 ± 0.48
928	0.81 ± 0.39	2.39 ± 0.52	0.84 ± 0.36	2.14 ± 0.59
929	0.82 ± 0.50	2.98 ± 0.90	0.57 ± 0.37	2.65 ± 0.80

Note: The most important change in carbonate accumulation occurs in the deepest site where the increase in accumulation since 433 ka must have resulted from greater preservation because of less corrosive bottom waters. This pattern implies that the $[CO_3^{-2}]$ gradient across the water mass boundary has decreased since 433 ka.

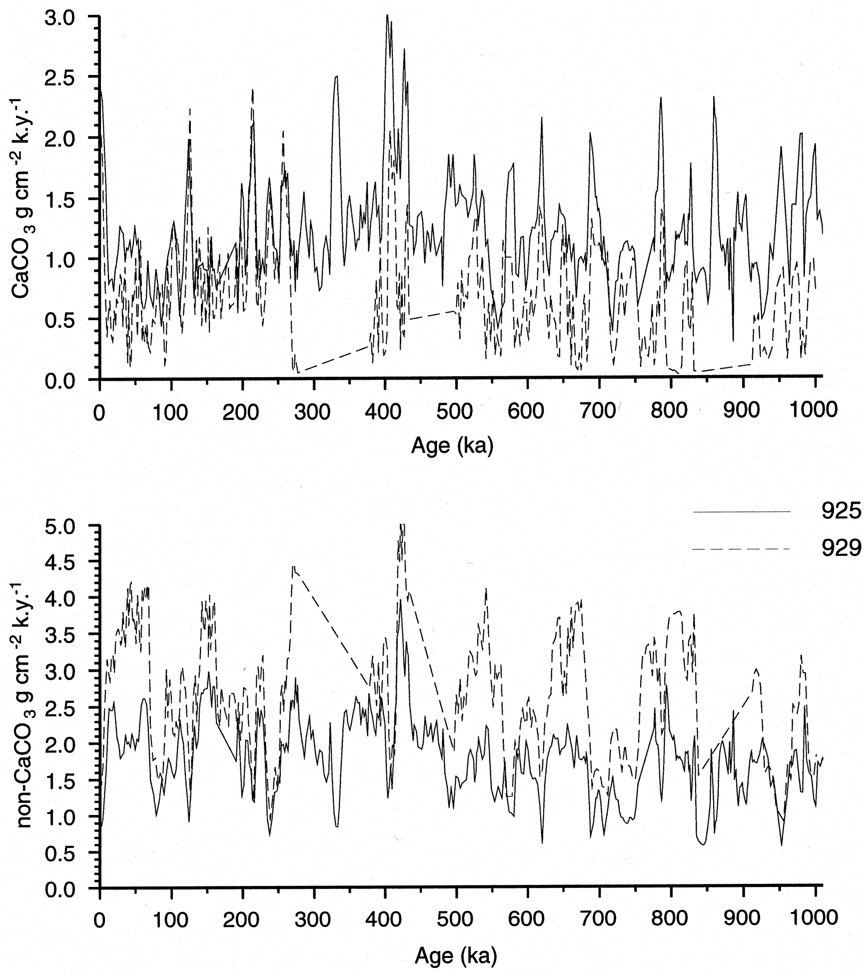

Figure 9. Carbonate and noncarbonate accumulation in the shallowest (925) and deepest (929) sites. Accumulation rates were calculated as the product of the instantaneous sedimentation rates in Figure 3, the estimated bulk density from Figure 8, and the measured carbonate concentration. Carbonate accumulation is much more similar in the two sites in the younger part of the record than in the older, suggesting that the rate of dissolution has decreased during the last 1 m.y. Productivity has varied significantly on short time scales, but long-term averages are nearly the same (see Fig. 10). The deepest site has always had greater accumulation of noncarbonate material. Also, there appears to have been an increase in noncarbonate accumulation, suggesting an increasing input of Amazon-derived material throughout the last 1 m.y.

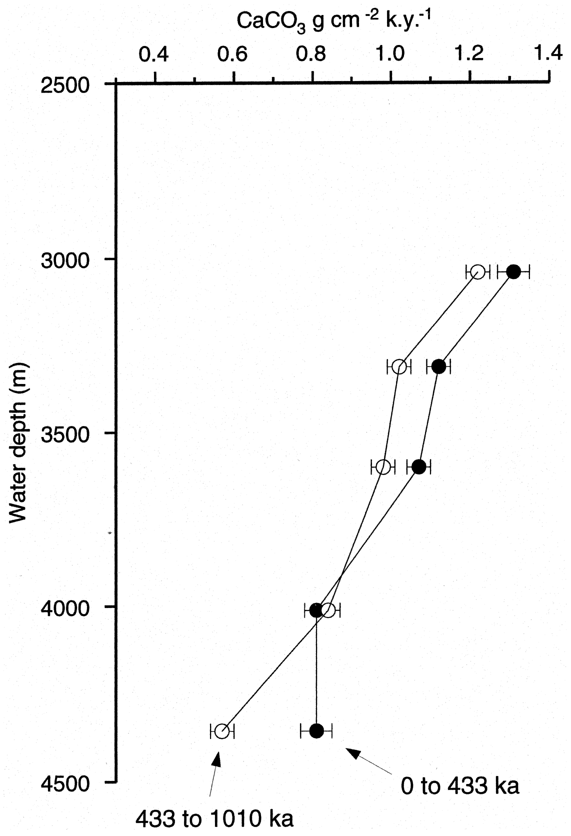

Figure 10. Averages of carbonate accumulation. The error bars are standard errors calculated as 1σ/√*n*. The patterns suggest that long-term variations in productivity have been small. The largest change in accumulation occurred in the deepest site and was the result of a decrease in dissolution in the younger part of the record. The text discusses several possible causes of this pattern of variation.